

Sustainable CO₂ Utilization as a Blowing Agent in Thermoset PHU Foam Production with Humidity-Responsive Shape Memory

Katherine Gouveia, Joshua Vauloup, Maxime Colpaert, Connie Ocando, Patrick Lacroix-Desmazes, Vincent Ladmiral, Sylvain Caillol,* and Jean-Marie Raquez*



Cite This: *ACS Appl. Polym. Mater.* 2025, 7, 6113–6124



Read Online

ACCESS |



Metrics & More



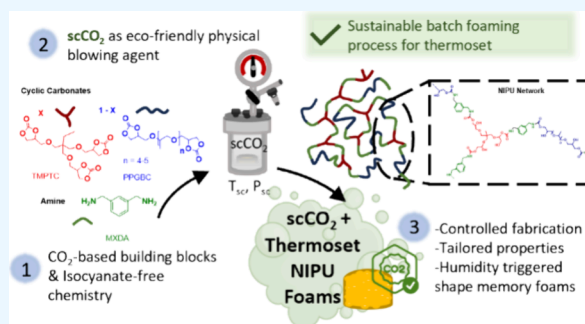
Article Recommendations



Supporting Information

ABSTRACT: Polyurethane (PU) foams are essential for energy-efficient insulation but are problematic due to the use of harmful isocyanates. Nonisocyanate polyurethanes (NIPUs) offer a safer, more sustainable alternative, aligning with EU regulations and climate goals. In this work, we report an eco-friendly method for producing thermosetting NIPU foams with tailored properties and humidity-responsive shape memory using supercritical CO₂ as a physical blowing agent. This innovative approach not only replaces current flammable, greenhouse-gas-emitting agents with high global warming potential but also revalorizes CO₂ in the manufacturing and synthesis process. The method involves CO₂ pressure-induced absorption, temperature-induced desorption, and curing of five-membered cyclic carbonate/amine resins. At elevated temperatures, simultaneous CO₂ release and NIPU cross-linking drive cellular structure formation. We studied the effects of curing agents, foaming/curing temperatures, and the impact of stabilizers on the final foam properties. The resulting foams demonstrated tunable densities (270–451 kg/m³), compression moduli (16–350 kPa), and cell sizes (0.33–0.99 mm). Notably, these NIPU foams also exhibited humidity-triggered shape memory behavior, which can greatly expand their functionality. This process ensures a controlled and sustainable approach to fabricating NIPU thermoset foams and represents a transformative step forward in the development of greener PU-based materials.

KEYWORDS: non isocyanate polyurethanes, supercritical CO₂, CO₂-based cyclic carbonates, amines, CO₂ revalorization



INTRODUCTION

Polyurethane foams (PUFs) have become indispensable in our daily lives, with an annual production of 20 Mt/year. They are extensively used in various applications, as both rigid and flexible materials, to enhance functionality and comfort in our society. PU cellular materials present extraordinary mechanical properties owing to their lightweight nature, thermal insulation, and energy absorption capabilities.^{1,2} Thanks to their straightforward manufacturing process and exceptional performance characteristics, PUFs have been widely exploited in various industries, ranging from the construction sector to furniture manufacturing.^{3,4} They significantly contribute to creating energy-efficient structures, as thermal insulation materials, and by elevating personal comfort in applications like bedding and cushioning. This wide range of applications is ascribed to the right selection of reagents, together with good process control, to finely adjust their morpho-structural properties to fulfill foam requirements.⁵

The fundamental chemistry of PUFs involves a reaction between isocyanates and polyols, with the addition of a blowing agent responsible for creating small cavities within the polymeric material.² In the industrial manufacturing process, two types of blowing agents are typically employed to produce

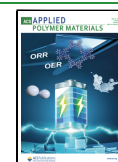
PUFs: chemical blowing agents (CBAs) and physical blowing agents (PBAs).⁶ CBAs are substances that undergo chemical reactions, triggered by the polymer's exothermic reaction, external heat, or polymer processing. These reactions produce gaseous byproducts, such as CO₂ and H₂, which create the porosity in the foam.⁷ For instance, self-blowing PUF is produced by adding water as a CBA to the reactive polyurethane formulation. This addition partially hydrolyzes isocyanates into carbamic acid, which quickly decomposes into urea and CO₂ in situ, creating the foam's porosity.² Hydrocarbons, such as pentane, isobutane, cyclopentane, chlorofluorocarbons (CFCs), and hydrofluorocarbons (HFCs), are common examples of PBAs. While these PBAs are effective in producing PU foams, hydrocarbons are highly flammable. Moreover, CFCs and HFCs were discontinued

Received: February 10, 2025

Revised: April 29, 2025

Accepted: April 30, 2025

Published: May 14, 2025



following the Montreal Protocol due to their classification as greenhouse gases having high global warming potential.^{2,6}

Despite the global demand for PUFs and their significant market size, estimated at \$49.5 billion in 2023, environmental and health concerns are rising due to the use of harmful isocyanates in their production.⁸ As a result, safer synthetic pathways, aligning with European legislations (REACH) and climate goals,⁹ have emerged to develop materials that chemically resemble conventional PUs. In this regard, the aminolysis reaction of biobased CO₂-derived five-membered cyclic carbonates, leading to polyhydroxyurethanes (PHUs), is deemed the safest synthetic pathway to produce PU-like foams, also known as nonisocyanate polyurethane (NIPU) foams.¹⁰

Among the pioneering works, Caillol and co-workers^{11–13} developed self-blown NIPU foams through the polyaddition of diamines and polyfunctional five-membered cyclic carbonates, in combination with the H₂ release provided by Momentive MH15, a poly(methylhydrogenosiloxane), used as a CBA. In Detrembleur's group, Monie et al,¹⁴ recently exploited decarboxylative S-alkylation, introducing thiols to the formulation to release CO₂ in situ. In view of simplifying the foaming process, they also fabricated NIPU foams through the addition of water to hydrolyze the five-membered cyclic carbonates and release CO₂ in situ.¹⁵ While self-blown NIPU foams using CBAs have been reported largely, the fabrication of NIPU foams with PBAs has been under-investigated. The use of PBAs provides numerous advantages, such as improved control over the foaming process and smoother surface finishes. Indeed, PBAs expand the polymeric matrices through vaporization, an endothermic process that allows for better control of the foaming process with more homogeneous expansion. Additionally, the quantity of PBAs can be adjusted in the formulation to achieve the desired foam characteristics such as density, cell size, etc. Moreover, PBAs do not chemically react with the polymeric matrix to produce gases and are generally chemically inert, reducing the risk of side reactions due to variations in temperatures, humidity, or other environmental and processing conditions.

Among these PBAs, scCO₂ is gaining increasing attention in both academic and industrial fields, particularly in the case of polymeric foams, including PU foams, due to their advantageous characteristics.^{16–19} CO₂ is abundantly available and considered a zero ozone-depletion substance. Furthermore, its recyclability, nontoxicity, and nonflammability render it highly attractive in industrial applications, being aligned with the principles of eco-friendly applications and processes.^{20,21} Grignard et al,²² successfully fabricated microcellular thermoplastic NIPU foams by bio-/CO₂-sourced NIPU films using supercritical CO₂ (scCO₂) conditions and quickly releasing the CO₂ at medium temperatures for 1 min and then stabilizing the porous material structure in a cold bath. Surprisingly, this unique method for fabricating thermoplastic foams has not been applied to other NIPU foams, especially thermoset foams, which are of greater interest in terms of volume and market demand.

Herein, we present an innovative eco-friendly and sustainable method for the fabrication of thermosetting NIPU foams by exploiting scCO₂ as a PBA in a batch process. This approach advances the field by addressing the challenge of simultaneously curing and foaming the NIPU network at moderate temperatures, which are crucial for producing PUF. This paper addresses these challenges by first examining the kinetics of reactive monomers at low temperatures using

reheology. The foaming process begins with the infusion of PHU material precursors with scCO₂. Foaming is then initiated by CO₂ desorption and simultaneous curing of the NIPU network at moderate temperatures. The study also explores the impact of curing agents (monomers), additives (nucleating agents and surfactants), and curing/foaming temperatures on the final morpho-structural and mechanical properties of the cellular materials.

Our method enables the creation of a series of rigid thermoset NIPU foams with adjustable properties and humidity-responsive shape memory materials (SMMs). Moreover, this approach leverages CO₂ not only through its incorporation in the synthesis of five-membered cyclic carbonates but also as a physical blowing agent. This represents a significant advancement toward greener alternatives and offers a promising emerging technology for the controlled fabrication of thermoset NIPU foams.

EXPERIMENTAL SECTION

Materials. Trimethylolpropane triglycidyl ether (TMPT) and tetrabutylammonium bromide (TBAB) (purity 99%) were purchased from Sigma-Aldrich (Darmstadt, Germany). Polypropylene glycol, α,ω bis(cyclocarbonate) (PPOBC) was acquired from Specific Polymers (France). M-xylylenediamine (MXDA) was purchased from TCI. Laponite, Tegostab E-8930, and Tegostab E-8158 were kindly supplied by Evonik. Ethyl acetate and tetrahydrofuran were purchased from VWR International S.A.S. The NMR solvent CDCl₃ was obtained from Eurisotop. CO₂ (Alphagaz CO₂ SFC, $\geq 99.998\%$) was purchased from Air Liquide.

Characterizations. *Nuclear Magnetic Resonance.* ¹H NMR spectroscopy experiments were performed using a Bruker Avance 400 MHz spectrometer at 25 °C. All ¹H NMR samples were dissolved in CDCl₃. Shifts are given in ppm.

Titration of the Carbonate Equivalent Weight by ¹H NMR. The carbonate equivalent weight (CEW, g eq^{−1}) was calculated by ¹H NMR. Benzophenone was used as an internal standard. In an NMR tube, known masses of monomer and benzophenone were introduced and dissolved in 600 μ L of CDCl₃. Then, the CEW = 191 eq mol^{−1} was determined using the following equation:

$$\text{CEW} = \frac{I_1 \times H_{\text{carbonate}}}{I_2 \times H_{\text{PhCOPh}}} \times \frac{m_{\text{carbonate}}}{m_{\text{PhCOPh}}} \times M_{\text{PhCOPh}}$$

where I_1 is the integration of the signal corresponding to CH of benzophenone (7.4 ppm), I_2 is the integration of the signal corresponding to CH of carbonate (4.8 ppm), $H_{\text{carbonate}}$ is the number of carbonate protons, H_{PhCOPh} is the number of protons related to benzophenone, $m_{\text{carbonate}}$ is the product mass, m_{PhCOPh} is the benzophenone mass, and M_{PhCOPh} is the benzophenone molar mass.

Fourier Transform Infrared Spectroscopy. Infrared spectra were recorded on a Bruker IFS 66v/S spectrometer equipped with an attenuated total reflectance (ATR) cell. Spectra were obtained in the transmission mode with 32 scans and 4 cm^{−1} resolution in the 600–4000 cm^{−1} range.

Differential Scanning Calorimetry. Differential scanning calorimetry (DSC) analyses were performed using a NETZSCH DSC200F3. Calibration was performed using indium under a N₂ flow. Approximately, samples of 5–6 mg were introduced in a pierced lid aluminum pan. The analyses were conducted at a heating rate of 10 °C/min between −40 and 150 °C. The dried foams were conditioned using a first ramp from 25 to 80 °C and a 5 min isothermal treatment at 80 °C. Then, the T_g values of the dried foams were measured from the second ramp.

Gel Content. Three samples of approximately 300 mg of the same foam were weighed and immersed in THF for 24 h. Consequently, the samples were dried under a vacuum at 70 °C for 16 h. The gel content (GC) was calculated using the following equation:

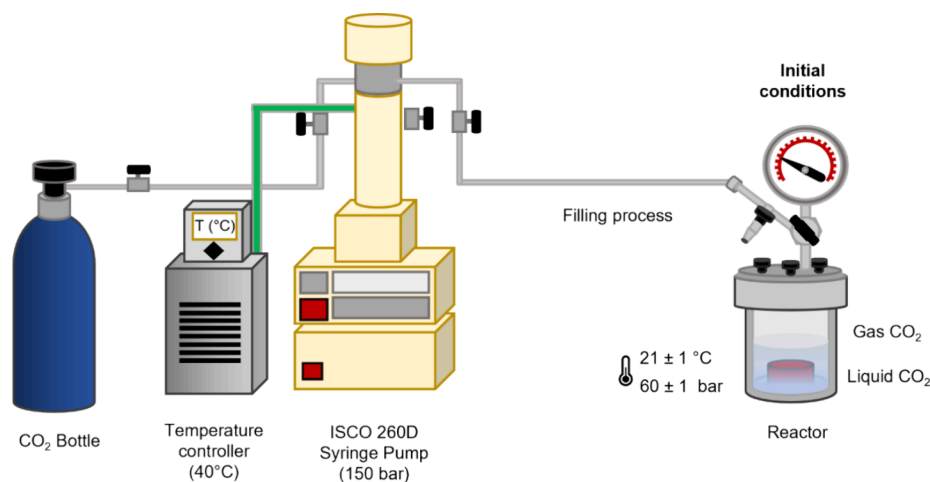


Figure 1. Experimental setup conditions to fill up the reactor with CO₂.

$$GC(\%) = 100 \times \frac{m_1}{m_0}$$

where m_0 is the initial mass of the foam sample before immersion and m_1 is the mass after immersion and drying.

Density. Density was assessed using a gravimetric method by cutting cubes of approximately 10 mm³. They were measured and weighed. The density was calculated by dividing the mass by the volume. Each foam density was measured in triplicate, and the density reported is the mean of the three measurements.

Water Uptake. Three samples of each foam were previously dried under a vacuum at 80 °C overnight and weighed (m_2). Then, the foams were placed in a desiccator with a saturated KCl solution with approximately 85% relative humidity for 48 h and weighed again (m_3). The water content (WC) percentage absorbed by the foams was calculated by the following equation:

$$WC = \frac{m_3 - m_2}{m_2} \times 100$$

The WC uptake over time in the SMM section was measured using thermogravimetric analysis, and the average value of three measurements is reported.

Scanning Electron Microscopy. NIPU foam cell morphology images were analyzed by using scanning electron microscopy (SEM). All of the images were acquired using an FEI QUANTA 200 FEG. The pore sizes were measured using ImageJ software.

Thermogravimetric Analysis. Thermogravimetric analyses were performed on a Netzsch TG 209TG 209F1 with a nitrogen flow of 40 mL min⁻¹ for the sample atmosphere (and 20 mL min⁻¹ nitrogen flow of protective gas for balance protection). Samples of around 10 mg were placed in an aluminum pan, and the weight loss was analyzed upon heating the samples from room temperature to 600 °C at a heating rate of 10 °C min⁻¹.

Compression Test. The compression tests were performed by using an INSTRON machine. Compression was done on cubic samples of around 1 cm³ at a fixed rate of 1 mm min⁻¹. The compression modulus was calculated using the beginning of the linear range of the stress–strain curve slope.

Recovery Ratio Percentage. The recovery ratio (R_r) of the NIPU foams was calculated from the different heights of the foam before and after recovery using the initial height (initial temporary shape) and recovered height upon exposure to humidity. The R_r was calculated using the following equation:

$$R_r(\%) = \frac{H_{\text{recovered}} - H_{\text{compressed}}}{H_{\text{original}} - H_{\text{compressed}}}$$

where $H_{\text{recovered}}$ is the height of the foam exposed to humidity over time, $H_{\text{compressed}}$ is the height of the foam after compression and before

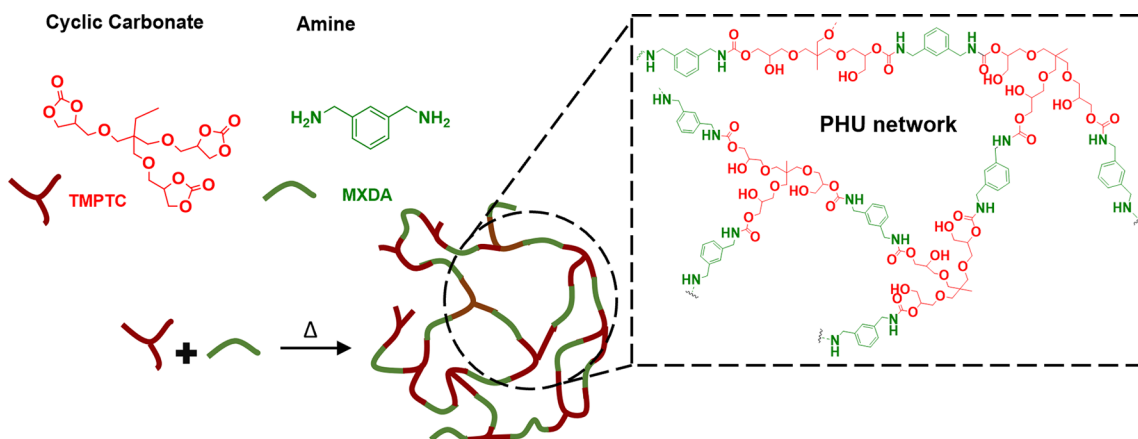
exposure to humidity, and H_{original} is the original height of the foam before being compressed.

SYNTHESES

Synthesis of 4,4'-(((2-Eethyl-2-(((2-oxo-1,3-dioxolan-4-yl)methoxy)methyl)propane-1,3-diyl)bis(oxy))bis(methylene))bis(1,3-dioxolan-2-one) (TMPTC). TMPT (150 g, 0.50 mol) was poured into a 600 mL hastelloy pressure reactor (Parr Instrument Company) with TBAB (3.75 g, 0.012 mol) and solubilized in 150 mL of ethyl acetate. The reaction was performed at 80 °C for 96 h at a constant CO₂ pressure of 20 bar. The crude solution was washed 3 times with water and 2 times with brine to remove TBAB. Magnesium sulfate was added to remove the residual water, and ethyl acetate was removed under vacuum at room temperature to obtain a yellowish viscous liquid (yield = 95%). CEW = 191 eq mol⁻¹. ¹HNMR (400 MHz, CDCl₃, ppm): δ = 0.84 (t, 3H, CH₃), 1.41 (m, 2H, CH₂–CH₃), 3.28–4.03 (m, 6H, Cq–CH₂), 4.46 (m, 3H, CH₂–O(C=O)–O), 4.49 (t, 3H, CH₂–O(C=O)–O), 4.85 (m, 3H, CH–O(C=O)–O) (Figure S1).

General Procedure for Thermoset NIPU Foam Fabrication Using scCO₂ as a Blowing Agent in the Batch Mode. Typically, a carbonate mixture (trifunctional and bifunctional) and additives (5 wt % Laponite relative to the total resin mass or 0.5 wt % additives relative to the cyclic carbonate mixture mass) were weighed and placed in a 5 mL plastic pot. This mixture was mixed for 3 min at room temperature in a speed mixer at 2500 rpm to obtain a homogeneous mixture. Then, the diamine was added to the carbonate mixture and mixed again in the speed mixer for 3 min at room temperature at 2500 rpm. The formulation was then transferred to a 27 mm diameter and 12 mm height open circular silicon mold (wall thickness = 1 mm). The mold was placed in a 100 mL stainless steel reactor (Parr Instrument Company) equipped with a 130 bar rupture disk and sealed. The reactor was then filled at room temperature (liquid CO₂) with 77 mL of CO₂ (vapor pressure of liquid CO₂ of about P = 59 ± 1 bar at T = 22 ± 1 °C in the reactor) using an ISCO syringe pump (model 260D) thermostated at 40 °C and operating under the constant pressure mode set at 150 bar (77 mL of CO₂ at 40 °C and 150 bar, and thus a CO₂ density of 0.78023 g/mL, corresponding to a delivered mass of CO₂ of 60.07 g²³) (Figure 1). Subsequently, the reactor was heated to

Scheme 1. Scheme Reaction of the PHU Formation Network and Structure of the Reagents for the Validation Foaming Process



45 °C to reach the scCO₂ domain with a final pressure of 100 bar. The sample was saturated with scCO₂ for about 90 min under these conditions. Then, the reactor was cooled to 0 °C with an ice bath and quickly depressurized (in about 2 min). Finally, the CO₂-saturated sample was heated in an oven under air at 80, 100, or 140 °C to effect the simultaneous temperature-induced CO₂ desorption and cross-linking processes.

RESULTS AND DISCUSSION

NIPU Foam Preparation. To validate and conduct the foaming process of our thermosets using scCO₂ as a blowing agent in a batch process, a reference formulation was selected to produce NIPU thermosetting foams. The initial solvent-free and catalyst-free NIPU thermoset formulation consisted of a five-membered tris(cyclic carbonate), trimethylolpropane triscarbonate (TMPTC), and an aromatic primary diamine, MXDA (Scheme 1). TMPTC was previously purified to remove TBAB, a catalyst used for the fixation of CO₂ into epoxides, which could catalyze the aminolysis reaction in the curing process. A fixed [TMPTC]/[MXDA] ratio of 1:1 (expressed in cyclic carbonate and amine equivalents, respectively) was used. These monomers are viscous liquids, ensuring easy mixing and high homogeneity.

It is important to recognize that the foaming process is complex and requires specific conditions. Viscosity and cross-linking degree are crucial parameters to consider when producing thermosetting cellular materials. Thermosetting foaming involves two concomitant processes at high temperatures to effectively produce foam materials: (i) the efficient cross-linking of the PHU network and (ii) the formation of the cellular structure due to the gas release. Kinetic differences between these processes could give rise to two undesired scenarios: (1) the formation of a highly cross-linked network before gas release (blowing agent), leading to a thermoset material, and (2) the rapid release of the gas before the formation of a cross-linked network, which would impede the trapping of CO₂, resulting in the collapse of the foam structure.¹⁴ These specific conditions, particularly the control of rheological parameters during cross-linking, have been reported to be essential for producing NIPU foams using self-blowing mechanisms.^{11,14,15,24} To successfully foam thermosetting materials, in our case, it is fundamental to study and control the conditions of the reactants for the high-pressure

CO₂ absorption step. This ensures the appropriate rheological conditions for better control of the subsequent steps, including both foaming and curing steps. The kinetics of the reactive mixture (TMPTC/MXDA) was analyzed by rheology at 45 °C, a temperature at which CO₂ surpasses its critical point (when $P > 74$ bar). The rheological curves are presented in Figure 2.

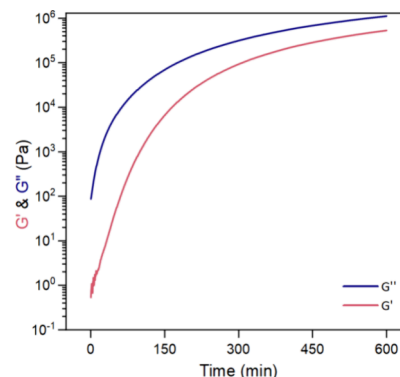


Figure 2. Rheological study of the G' and G'' between TMPTC and MXDA. **Conditions:** [TMPTC]/[MXDA] = 1/1 (expressed in equivalent functions), $T = 45$ °C, $t = 10$ h.

The absence of gel point (related to the crossover between G' and G'') suggests that after 10 h, the reactivity of the MXDA toward TMPTC is low enough to keep the SCC/amine formulation uncured. This allows CO₂ to diffuse into the not-yet cross-linked mixture. The impregnation step and foaming process depend on the remaining material to be expandable after CO₂ absorption at 45 °C. Therefore, scCO₂ conditions of 45 °C and 100 bar were used to facilitate the absorption in the reactor. The method used here consists of two main steps. One is the CO₂ pressure-induced absorption followed by CO₂ temperature-induced desorption as depicted in Figure 3. For the first step, the uncured mixture of the five-membered cyclic carbonate with diamine (SCC/amine) was placed into a reactor under scCO₂ conditions (T_{sc} ; P_{sc}) to assist with CO₂ absorption into the sample. The temperature (T_{sc}) and pressure (P_{sc}) were held constant for a period of time to allow proper CO₂ diffusion through the sample. It is important to note that primary amines can chemically interact with CO₂, forming reversible carbamate salts and carbamic

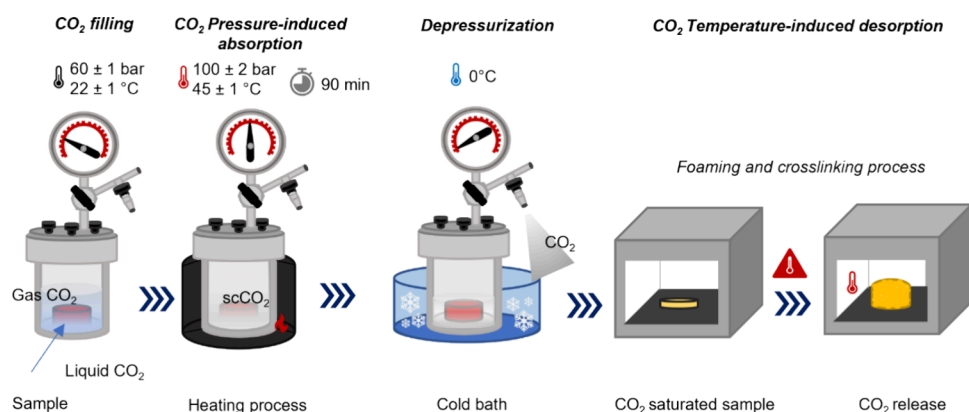


Figure 3. Scheme for the strategy for the thermosetting NIPU foaming process using scCO_2 as a blowing agent.

acid under mild conditions.²⁵ These reactions enhance CO_2 capture and, due to their reversible nature, contribute to gas release upon heating above 100 °C. The formation of carbamate species under supercritical conditions was confirmed by the appearance of characteristic peaks at 1545 cm^{-1} (COO^- carbamate), 1664 cm^{-1} (C=O carbamic acid), and 2206 cm^{-1} (physically adsorbed CO_2) in the FTIR spectrum^{26,27} (see Figure S2).

After the saturation stage, the reactor was cooled to 0 °C with a cold bath (at this temperature, CO_2 is liquid, and its vapor pressure is about 35 bar) and quickly depressurized to keep the CO_2 fixed into the sample. By doing so, the foam expansion is not dependent on the depressurization rate, as explained in Grignard's previous work on thermoplastic NIPU foams.²² A subsequent thermal step was then required to obtain a well-defined and stable cellular structure. The CO_2 -saturated SCC/amine formulation was heated at moderate temperatures (100–140 °C) to induce CO_2 release and promote curing of the SCC/amine resin simultaneously.

Four foams were synthesized using TMPTC and MXDA, with and without additives (Laponite), saturated under scCO_2 conditions (T_{sc} : 45 °C; P_{sc} : 100 bar) for 1.5 h, followed by a foaming step (100–140 °C). Table 1 presents the conditions

Table 1. Foaming Conditions for the Fabrication of NIPU Foams Using TMPTC and MXDA^a

entry	foaming temperature (°C)/time (h)	additives
1	140/2 h	-
2	100/3 h	-
3	140/2 h	5 wt % Laponite
4	100/3 h	5 wt % Laponite

^aConditions: $[\text{TMPTC}]/[\text{MXDA}] = 1/1$ (expressed in equivalent functions of cyclic carbonates and amines); scCO_2 saturation conditions: $T_{\text{sc}} = 45$ °C and $P_{\text{sc}} = 100$ bar.

of the foaming process. Two foams, entries 1 and 2, were successfully synthesized without any additive and foamed at 140 °C for 2 h and 100 °C for 3 h, respectively. The obtained foams are presented in Figure 4A. Accordingly, the foaming mechanism can be described as follows. During the foaming step, CO_2 desorption is triggered, originating from both the physically absorbed gas in the SCC/amine matrix and chemically captured CO_2 associated with the unreacted amine groups. This initiates the nucleation and growth of gas bubbles, which begin at the surface (due to localized heat transfer) and progressively propagate throughout the material.

This early stage is visually evidenced to be transitioning from a translucent film to a white material within the first few minutes of heating, which corresponds to the formation of small gas cells. As heating continues, the bubbles are still able to expand due to CO_2 diffusion and the low cross-linking density of the uncured matrix. Simultaneously, the thermal decomposition of carbamate salt releases CO_2 , regenerating free amine groups, which enables further progression of the curing reaction (Figure S3). The increase in viscosity and cross-linking density ultimately stabilizes the cellular structure by trapping the gas within the polymer network.

Moreover, 5 wt % Laponite (relative to the total resin mass), a commercially available clay, was incorporated into the formulations (entries 3 and 4). This clay filler acts as a nucleating agent that improves the cellular morphology of the foams by reducing the pore sizes and increasing the nucleation sites for bubble formation. The Laponite addition was also expected to increase the formulation viscosity, aiding the trapping of the physical blowing agent within the polymer matrix during the initial stage of thermal treatment when the cross-linking extent was still low.^{14,24} For instance, a significant reduction in the cell size was observed at 140 °C by decreasing from 1.58 ± 0.73 mm without Laponite (see entry 1) to 0.58 ± 0.39 mm when Laponite was employed (entry 3). Moreover, a substantial decrease in the material density (by comparing the height of both foams) was visually noticed, as shown in Figure 4A.

The positive impact of Laponite on controlling cellular morphologies was even more evident at lower temperatures, specifically at 100 °C. The resulting foams (entry 4) did not show large voids or collapsed walls, unlike the foams without Laponite (Entry 2). As already reported elsewhere, 5 wt % laponite significantly enhanced the quality of the foams and led to a reduction of density of the material.²⁴ The FTIR analyses of the foams (Figure 4B) confirmed the formation of PHU by the appearance of the C=O peak band attributed to the urethane group at 1694 cm^{-1} and the disappearance of the cyclic carbonate band C=O at 1790 cm^{-1} corresponding to the starting TMPTC. Even though foams were successfully synthesized using this innovative method, further investigation into the foaming process is envisaged by tuning the monomer formulation. The same foaming process was conducted using TMPTC and an aliphatic amine hardener, specifically with Jeffamine EDR-148. The formulations were prepared with 5 wt % Laponite and without any additives. Foaming was induced at different temperatures (100, 120, and 140 °C). However, the

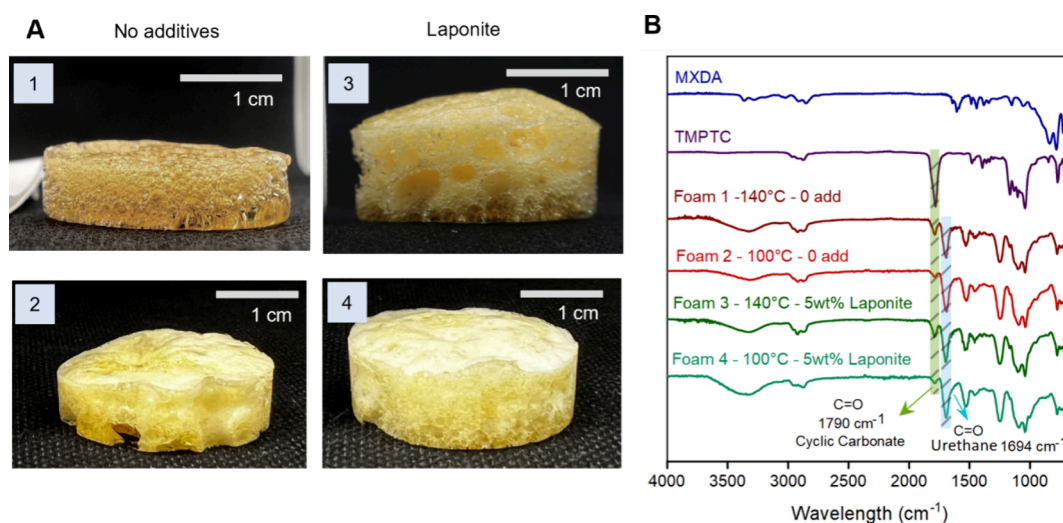


Figure 4. (A) Optical characterization of thermoset NIPU foams synthesized under scCO₂ in a batch process between TMPTC and MXDA. Foams 1 and 2 were synthesized without additives. Foams 3 and 4 were synthesized with 5% Laponite. **Conditions:** All foams were saturated under scCO₂ for 1.5 h at $T_{sc} = 45\text{ }^{\circ}\text{C}$ and $P_{sc} = 100\text{ bar}$. Foams 1 and 3 were foamed at $140\text{ }^{\circ}\text{C}$. Foams 2 and 4 were foamed at $100\text{ }^{\circ}\text{C}$. (B) FTIR spectra of the different NIPU thermoset foams.

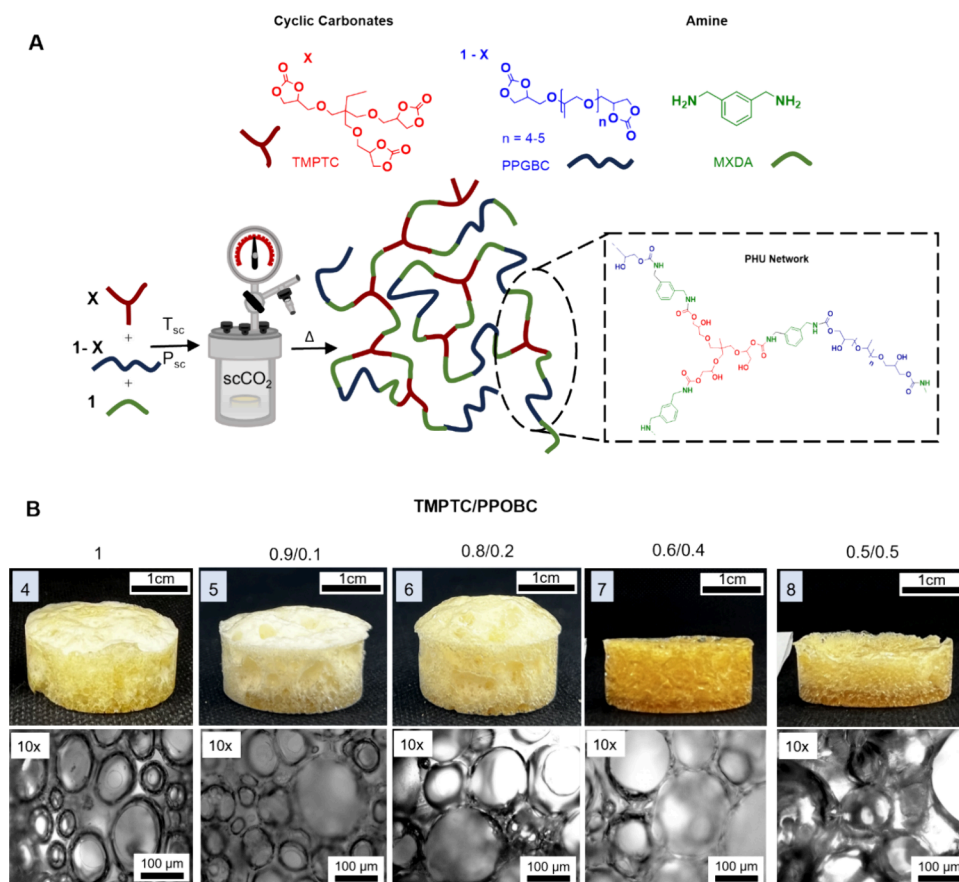


Figure 5. Visual characterization of NIPU foams obtained by varying the mass ratio of TMPTC and PPOBC versus amines (MXDA) in the formulation. All foams were loaded with 5 wt % Laponite and saturated under scCO₂ for 1.5 h at $T_{sc} = 45\text{ }^{\circ}\text{C}$ and $P_{sc} = 100\text{ bar}$ and foamed at $100\text{ }^{\circ}\text{C}$ for 3 h. FTIR spectra of the foams are presented in Figure S6.

resulting foams were not homogeneous. Visual characterization suggested that cross-linking occurred prior to the release of CO₂ (see Figure S4). Therefore, it was decided to continue the study with the formulation of TMPTC and MXDA.

Monomer Choice for Foaming Control. To better control the foaming process and enhance the morphology of

the cellular materials, it is crucial to carefully select the reactants in the formulation. Indeed, the choice of monomers has a significant influence on the resin mixture viscosity, curing rate, cross-linking density, and thermal and mechanical properties. The use of a cross-linking monomer is essential for obtaining homogeneous and well-structured foams. The

tris(5-membered cyclic carbonate), TMPTC, used in the previous section results in highly compact cross-linked rigid foams due to the short aliphatic chains of the TMPTC monomer. Caillol and co-workers¹² demonstrated that bis(cyclic carbonates) can impart flexibility to self-blown nonisocyanate PUFs, thereby enhancing their morphostructural properties. We thus decided to introduce a bis(5-membered cyclic carbonate), poly(propylene oxide) biscarbonate (PPOBC), with a polyether backbone to confer flexibility to the foams (Figure 5A). A series of different formulations was accordingly prepared by varying the mass ratio of the trifunctional (TMPTC) and bifunctional cyclic carbonates (PPOBC) while keeping the equivalence of functions between cyclic carbonates and amines constant and equal to 1 (i.e., $([\text{TMPTC}] + [\text{PPOBC}])/([\text{MXDA}]) = 1/1$) (Table 2).

Table 2. NIPU Foam Formulations with 5 wt % Laponite and Main Characteristics of Thermoset NIPU Foams Obtained by scCO₂ Saturation at $T_{\text{sc}} = 45\text{ }^{\circ}\text{C}$ and $P_{\text{sc}} = 100$ bar for 1.5 h and Foaming at $100\text{ }^{\circ}\text{C}$ for 3 h

entry	[TMPTC] ^a	[PPOBC] ^b	density (g cm ⁻³)	T_g (°C)	GC ^c (%)
4	1	0	0.227 ± 0.047	49	97
5	0.9	0.1	0.296 ± 0.048	44	96
6	0.8	0.2	0.285 ± 0.025	40	94
7	0.6	0.4	0.491 ± 0.004	34	88
8	0.5	0.5	0.338 ± 0.037	28	85

^aTMPTC, trimethylolpropane triscarbonate. ^bPPOBC, poly(propylene oxide) biscarbonate. ^cGC, gel content.

Similar to our previous samples, these NIPU foam formulations were loaded with 5 wt % Laponite to control the foam morphology, followed by the same CO₂ pressure-induced absorption procedure. Then, the second step, CO₂ temperature-induced desorption, was carried out at $100\text{ }^{\circ}\text{C}$ for 3 h. The foams obtained from this study are depicted in Figure 5B.

Consistent with previous studies, incorporating PPOBC into the formulation altered the morphology and properties of the foams. The glass-transition temperature (T_g) of the foams exhibited a decrease when the content of bis(cyclic carbonate) (PPOBC) was increased. Employing only TMPTC in the formulation (entry 4) yielded a T_g of $49\text{ }^{\circ}\text{C}$, in contrast to the T_g of $28\text{ }^{\circ}\text{C}$ observed for a 0.5/0.5 TMPTC/PPOBC ratio (entry 8). DSC thermograms are presented in Figure S5. The GC of these foams was also assessed (Table 2). The GC of the foams prepared with a TMPTC mass fraction higher than 0.8 was rather high (GC > 94%), indicating highly insoluble networks and confirming the cross-linking process between the

triscarbonates and diamines. Indeed, GC values of 97, 96, and 94% were obtained with 100% TMPTC (entry 4), 0.9/0.1 TMPTC/PPOBC (entry 5), and 0.8/0.2 TMPTC/PPOBC (entry 6), respectively. When a higher quantity of PPOBC biscarbonate was added, a decrease in GC was noticed. For instance, GCs decreased to 88 and 85% for 0.6/0.4 TMPTC/PPOBC (entry 7) and 0.5/0.5 TMPTC/PPOBC (entry 8), respectively. The material density was also measured to complement the visual characterizations shown in Figure 5. The foam densities ranged from 0.227 to 0.491 g cm⁻³. Entries 7 and 8 exhibited the highest density values, $0.491 \pm 0.004\text{ g cm}^{-3}$ and $0.338 \pm 0.037\text{ g cm}^{-3}$, respectively.

In this case, a higher amount of PPOBC decreases the viscosity of the reactive mixture and extends the gelation time (defined as the crossover of G' and G''). With 100% TMPTC at $80\text{ }^{\circ}\text{C}$, gelation occurred in 48 min; however, when 0.2 mass fraction of PPOBC was added, the gelation time increased to 75 min, and with 0.5 mass fraction of PPOBC, the gelation point was delayed significantly to 319 min. This slower cross-linking rate and reduced viscosity hinder the effective trapping of the blowing agent (CO₂) during the curing process (see Figure S7). Entries 5 and 6 (Table 2) resulted in densities of 0.296 ± 0.048 and $0.285 \pm 0.025\text{ g cm}^{-3}$, respectively. Based on this assessment, a 0.8/0.2 TMPTC/PPOBC formulation (entry 6) was selected as the most promising candidate for further foaming investigation.

Tuning NIPU Foam Properties. Additives are essential for manufacturing tunable foams and precisely controlling the foaming process. They offer various advantages including enhancing overall morphological stability and influencing mechanical properties through viscosity, cell size, and density adjustment.^{5,28} These benefits allow for precise control over the final foam's characteristics and applications. In the production of morphologically stable thermosetting NIPU foams using scCO₂ as a PBA, it is necessary for the SCC/amine formulation to exhibit sufficient reactivity and viscosity during the foaming stage. This reactivity is essential for both trapping CO₂ and facilitating cross-linking. Given the rapid CO₂ thermally induced desorption observed in our study, the incorporation of additives became fundamental for enhancing the cellular expansion and avoiding the coalescence of the cellular material. To demonstrate the robustness of the foaming process and evaluate the characteristics and properties of the final foams, various additives were incorporated into the foam containing 0.8/0.2 TMPTC/PPOBC (entry 6). Alongside the synthetic clay (Laponite), two other additives, Tegostab E-8930 and Tegostab E-8158, were selected. Tegostab additives are surface-active agents with cell-regulating properties that reduce the interfacial tension generated during cell expansion, contributing to the stabilization of the foam.⁵

Table 3. Properties and Morphological Characterization of Thermoset NIPU Foams with Different Additives and Foaming Temperatures

entry ^a	foaming temperature/time	additives	GC (%)	density (g cm ⁻³)	cell size (mm)	$T_{\text{d5\%}}$ (°C)
9	100 °C/3 h		90	0.274 ± 0.048	0.42 ± 0.26	251
10	100 °C/3 h	5 wt % Laponite	94	0.285 ± 0.034	0.33 ± 0.16	260
11	100 °C/3 h	0.5 wt % E-8158	93	0.360 ± 0.014	0.59 ± 0.22	268
12	100 °C/3 h	0.5 wt % E-8930	94	0.451 ± 0.023	0.99 ± 0.37	260
13	140 °C/2 h	5 wt % Laponite	99	0.387 ± 0.010	0.91 ± 0.35	260
14	80 °C/1 h–120 °C/2 h	5 wt % Laponite	93	0.294 ± 0.032	n.d. ^a	260

^aAll foams were formulated with 0.8 TMPTC/0.2PPOBC/MXDA. CO₂ saturation conditions: T_{sc} : $45\text{ }^{\circ}\text{C}$ and P_{sc} : 100 bar for 90 min.

The foam formulation characteristics are summarized in Table 3. For this series of NIPU foams, the scCO₂ foaming protocol used for the 0.8/0.2 TMPTC/PPOBC formulation (Foam 6) was again employed. All of the formulations (0.8/0.2 TMPTC/PPOBC) with and without additives resulted in thermoset NIPU foams, as illustrated in Figure 6.

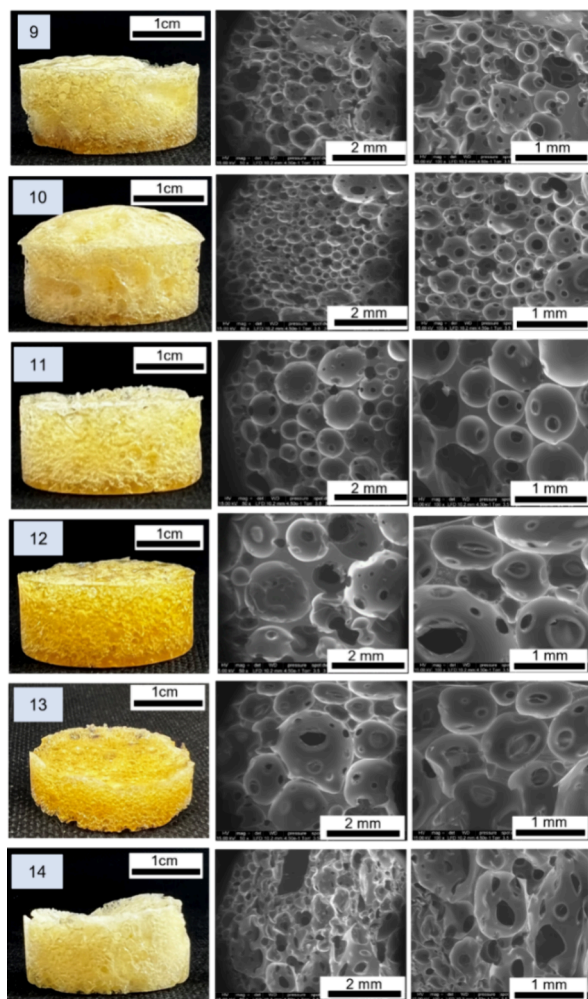


Figure 6. Pictures and SEM characterizations of thermoset NIPU foams synthesized from 0.8/0.2 TMPTC/PPOBC and MXDA with different additives and different curing/foaming temperatures. Foam 9 was without additives (reference). Foam 10 was with 0.5 wt % TEGOSTAB E-8158. Foam 11 was with 0.5 wt % TEGOSTAB E-8930. Foams 10, 13, and 14 were with 5 wt % Laponite. **Conditions:** Foams 9, 10, 11, and 12 were foamed at 100 °C for 3 h. Foam 13 was foamed at 140 °C for 2 h, and Foam 14 was foamed at 80 °C for 1 h. All foams were saturated under scCO₂ for 1.5 h at $T_{sc} = 45$ °C and $P_{sc} = 100$ bar in the reactor.

The morphologies of the foams and cell sizes were determined by SEM to assess the impact of these additives on the morpho-structural properties. All foams presented microcellular spherical closed pores with small localized cavities on the faces of the foams. To better showcase the effect of these additives on the formulation, a reference foam (entry 9) was designed without any additives. As observed in Figure 6, a material of relatively poor structural quality was formed.

As expected, adding 5 wt % Laponite to the formulation (entry 10) resulted in a decrease of the cell size, from $0.42 \pm$

0.26 (without additives) to 0.33 ± 0.16 mm (with Laponite), with a limited increase of the density, from 0.274 to 0.285 g cm⁻³. The formulation loaded with Tegostab E-8158 (entry 11) resulted in a high-density foam (0.360 ± 0.014 g cm⁻³) with a higher average cell size (0.59 ± 0.22 mm). When Tegostab E-8930 was incorporated into the formulation (entry 12), the cell size was significantly increased (0.99 ± 0.37 mm), and a high-density foam (0.360 ± 0.014 g cm⁻³) was formed. This behavior can be explained by the production of thicker walls between the large cavities (Figure S8). Importantly, the addition of these additives could tune the cell size of the foams. The results are depicted in Figure 7A.

The temperature effect on the CO₂-induced temperature desorption step was further studied on the formulation containing 0.2/0.8 TMPTC/PPOBC, loaded with 5 wt % Laponite and foamed at 100 °C (Foam 10). Two foams were synthesized at 140 and 80 °C, entries 13 and 14, respectively. The foams obtained are shown in Figure 6. Increasing the foaming temperature to 140 °C (entry 13) resulted in a denser foam (0.387 ± 0.010 g cm⁻³) with twice the average cell size (0.91 ± 0.35 mm) in comparison to entry 10, foamed at 100 °C. When the foaming temperature was decreased to 80 °C (Entry 14), the cellular material was of poor quality with a density of 0.294 ± 0.032 g cm⁻³. Results are displayed in Figure 7A. For the latter foam, the average cell size was not measured due to the heterogeneity of the cells, which might be caused by different rates of CO₂ release and curing.

The GCs were also evaluated (Table 3). The NIPU foams synthesized at a foaming temperature of 100 °C had high GC ranging from 90 to 94%, confirming the effective cross-linking of the SCC/amine mixture into a PHU network. The urethane group formation was also confirmed by FTIR analysis (see Figures S9 and S10). When the foam was produced at a higher temperature, i.e., 140 °C (entry 14), the GC was over 99%.

The T_g values of the dried foams (dried overnight) were determined by DSC. All of the results are summarized in Figure 7A, and DSC thermograms are presented in Figures S11 and S12. The T_g values of all of the NIPU foams were all within 35 and 42 °C and were not significantly affected by the additives or by the foaming temperature used. However, the polyaddition of cyclic carbonates and amines results in PHU networks containing hydroxyl groups due to the formation of hydroxyurethanes, rendering the foams hygroscopic.²⁹ To further explore the hydrophilic behavior, the water uptake of the foams was thereby determined. Overall, the NIPU foams scarcely absorbed 3–7 wt % water, which is consistent with previous studies on PHU foams and thermosets^{15,30} exposed to 50% RH. Despite this small WC, there was a significant impact on the thermal properties. For instance, the T_g of the NIPU foam, employing 0.2/0.8 TMPTC/PPOBC, loaded with 5 wt % Laponite and foamed at 100 °C (entry 10), significantly decreased from 35 °C (dried) up to -4 °C (moist). All of the NIPU foams followed the same trend, with the T_g of the moist foams ranging from -4 to 2 °C as shown in Figure 7A,B. (DSC thermograms are depicted in Figures S13 and S14.) This highlights the significant plasticizing effect of water on PHU networks by using only a small amount of water. Remarkably, when the foams were dried again, they recovered their initial T_g .

To evaluate the impact of additives on the properties of the NIPU foams, additional thermogravimetric analyses and compression testing were conducted. In the case of thermogravimetric analyses, all samples presented similar

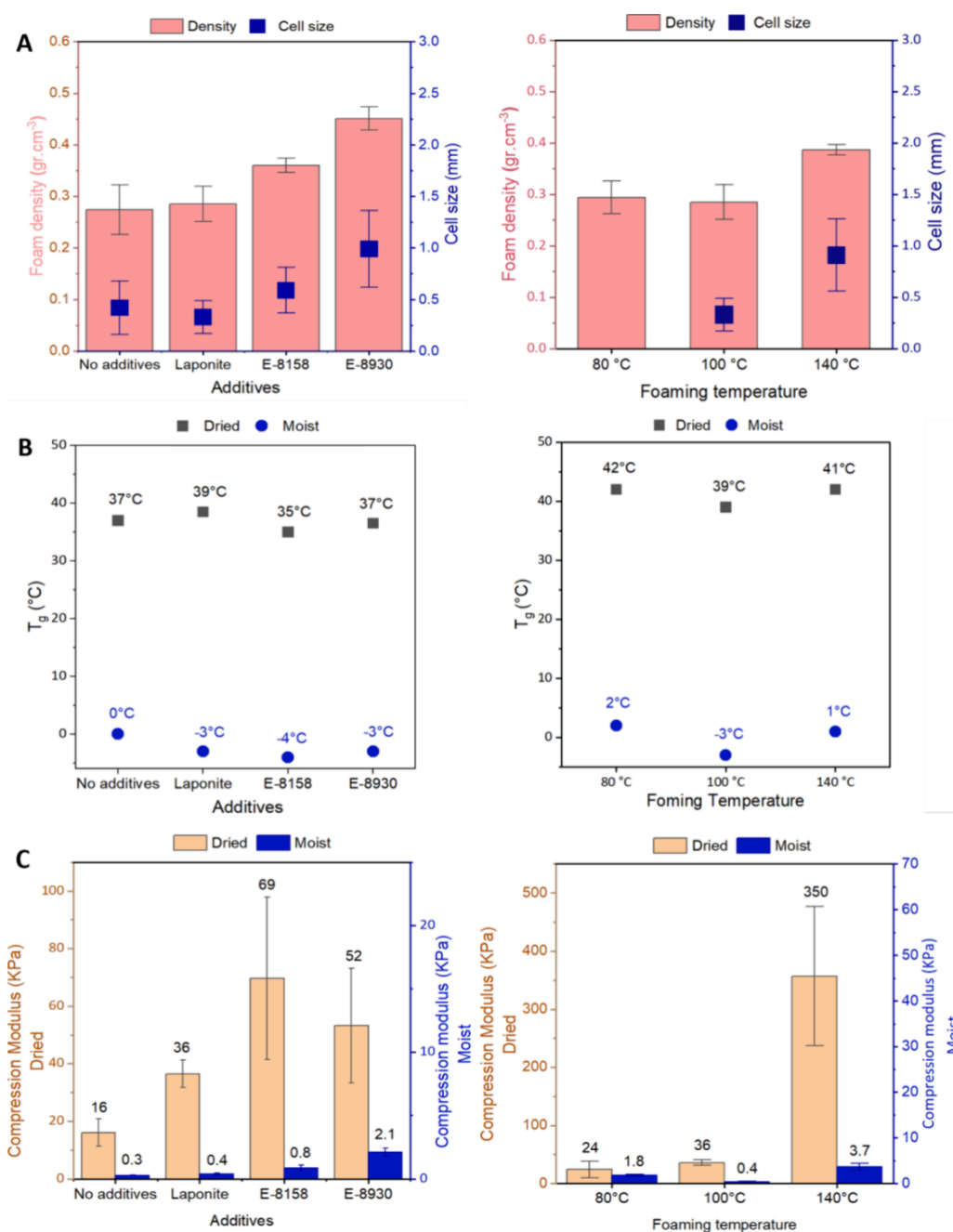


Figure 7. Foam density, cell size, and thermo-mechanical properties of NIPU foams. (A) Effect of the additives and CO₂ desorption temperatures on foam density and cell size. (B) T_g of the NIPU foams and effect of water. (C) Compression modulus of the NIPU foams in the dried and moist state.

degradation temperatures ($T_{d5\%}$) around 260 °C (Table 2), confirming that the additives did not influence the degradation temperature of the foams. All TGA thermograms are presented in Figures S15 and S16. This degradation temperature is even in the same range (250–300 °C) as previously reported in self-blown and physically blown PHU foams.^{12,14,15,29,31}

The impact of these additives was more highlighted in the case of the mechanical properties of NIPU foams by using compression tests (Figure 7C). All compression stress–strain curves are presented in Figures S17–S20. The foam synthesized without additives (Foam 9, dried) and characterized by the lowest density (0.274 g cm⁻³) exhibited the lowest compression modulus (16 kPa).

When the foam was added with 5 wt % Laponite (entry 10, dried) with a similar density (0.284 g cm⁻³), the compression modulus rose to 36 kPa. Importantly, the addition of the synthetic nanoclay to the formulation notably reinforced the mechanical strength of the cellular material under compression at comparable densities. When Tegostab E-8158 and E-8939 were used as surfactants in the foams produced at 100 °C, it resulted in compression moduli of 69 and 52 kPa, respectively. However, due to the considerable variation in foam densities (0.274–0.451 g cm⁻³), direct comparison of the compression modulus across all foams is not feasible. For instance, when the foaming temperature was modified to 80 and 140 °C for the foams containing 5 wt % Laponite, the compression moduli

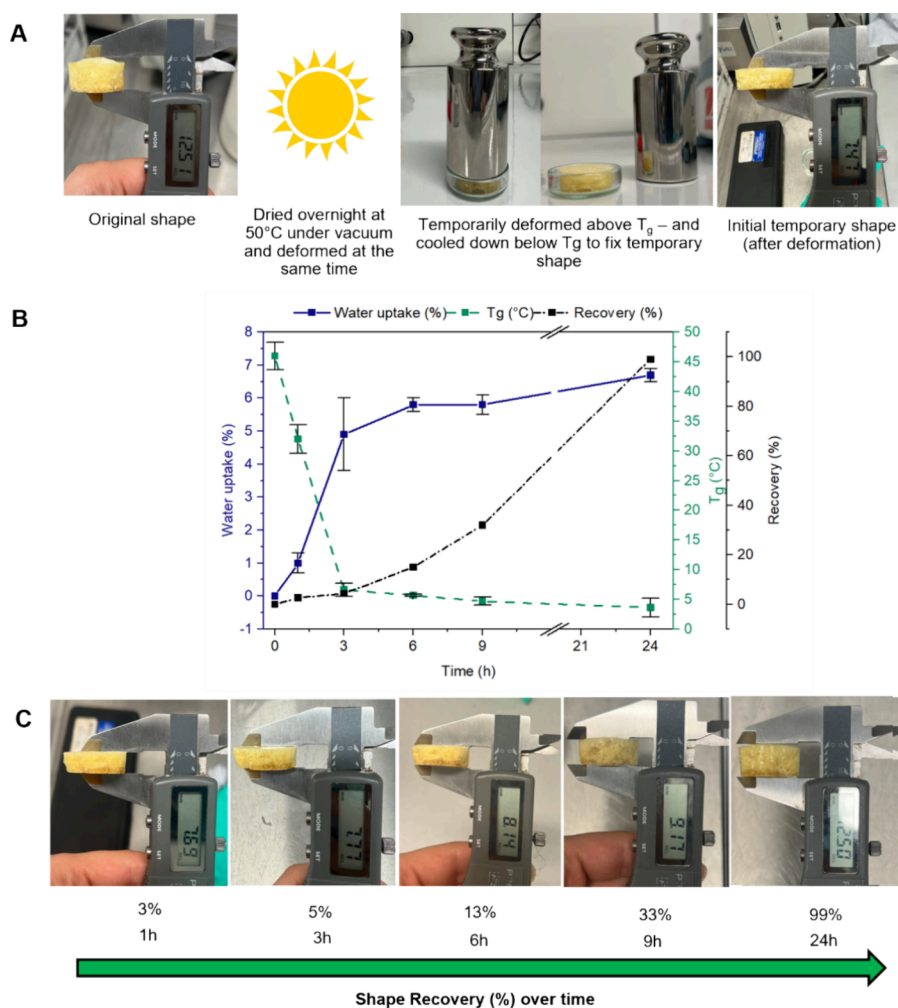


Figure 8. (A) Procedure to lock in the initial shape of the NIPU foam to study the shape memory behavior triggered by humidity. (B) Relationship among water uptake (%), T_g (°C), and shape recovery (%) over 24 h at 85%RH at room temperature. (C) Shape recovery triggered by humidity over time.

were measured at 350 kPa (entry 13, dried) and 24 kPa (entry 14, dried) (see Figures S21 and S22 for compression stress–strain curves).

As anticipated from the thermal properties, the mechanical properties were significantly influenced by water uptake and its plasticization effect. All of the moist foams exhibited a significant decrease in compression modulus by comparison to their dried counterparts. For instance, the compression moduli of moist foams (entries 9 and 10) were 0.03 and 0.04 kPa, respectively. Similarly, entries 11 and 12, in their moist state, exhibited reduced compression moduli from 69 to 0.8 kPa and from 52 to 2.1 kPa, respectively. Foam 13 also showed a decrease in the compression modulus from 350 to 3.7 kPa when moist. Compression curves of the moist foams are depicted in Figures S23–S28. These results demonstrate that water uptake leads to significant plasticization, which greatly reduces both the T_g and compression moduli compared to the dried foams. Even though this plasticization might be perceived as a drawback, it could actually be beneficial when these rigid foams are deemed as SMMs triggered by humidity. This affords an interesting approach to span the range of NIPU applications into advanced applications such as heart valves in the biomedical realm.³² To control the performance and behavior of these humidity-responsive foams, the relationship

among T_g , water uptake, and the shape recovery with time must be better understood, particularly by investigating the recovery of their original shape when exposed to moisture. To demonstrate the humidity-triggered shape memory effect, the NIPU foam, without any additive (entry 9), was dried overnight under vacuum to remove any remaining water at 50 °C. This additive-free foam was selected to study only the neat polymer behavior. The foam was heated at 60 °C and temporarily compressed, followed by rapid cooling to fix the shape ($H_{\text{compressed}}$) (see Figure 8A). The temporarily deformed foam was exposed to 85% relative humidity, and the T_g , water uptake, and Rr were measured with time. Figure 8B illustrates the evolution of these parameters with time. During the initial 3 h exposure of the NIPU foam to humidity, the water uptake reached 5 wt %, the T_g significantly decreased from 45 to 6 °C, and the foam recovered only 3% of its height. After 24 h, the water uptake increased to 7 wt %, the T_g remained stable (6 °C), and the foam recovered its initial height, reaching an Rr of 99% as depicted in Figure 8C. This experiment showed that the Rr rapidly evolves once the T_g goes below room temperature, indicating the material's excellent ability to recover its original shape. This behavior is consistent with the mechanism of shape memory polymers, where the external stimulus is moisture absorption and the T_g serves as the

switching parameter. In the dry state, the foam exhibits a T_g above room temperature, making the material rigid and capable of fixing a temporary shape. When the foam is exposed to humidity, water molecules are absorbed into the polymer matrix, forming hydrogen bonds with hydroxyl (–OH) and amino (–NH–) groups present in the PHU matrix.^{33,34} These interactions act as a plasticizer, lowering the T_g below room temperature. As a result, the foam transitions from a glassy to a rubbery state, allowing the polymer chains to regain flexibility and mobility. This enables the material to recover its original shape. Notably, a similar humidity-triggered shape memory mechanism has been reported in starch-based films, where the absorbed water also depresses the T_g and facilitates shape recovery.^{34,35} These moisture-triggered SMMs are particularly advantageous because they do not require any external energy source and are responsive to common environmental conditions.

CONCLUSIONS

We have developed an innovative and versatile strategy for the eco-friendly preparation of NIPU thermoset foams using scCO_2 as a physical blowing agent. This method is a safer and greener alternative to conventional blowing agents used in PUFs. The foaming strategy involves a two-step batch process. First, the uncured SCC/amine resin is impregnated with scCO_2 through a pressure-induced absorption step, followed by a CO_2 temperature-induced desorption step that occurs simultaneously with curing. In the second step, the rapid release of CO_2 coincides with the formation and cross-linking of the cellular material. Rheological measurements showed that the aminolysis of the diamine (MXDA) by the tri(cyclic carbonate) (TMPTC) at a low temperature (45 °C) was slow enough to maintain a slightly cross-linked resin before the release of CO_2 , allowing the resin to expand and create cellular cavities during the CO_2 desorption step. The proof of concept for the NIPU thermoset foaming process was successfully validated by fabricating rigid foams at different foaming/curing temperatures. After optimizing the formulation, the introduction of 0.2 mass fraction equivalent of 5-membered bis(cyclic carbonate) (PPOBC) to the formulation enhanced the homogeneity and structural integrity of the foams. This process and the optimized foam formulation allowed for the production of widely tailored and tunable foams by foaming/curing at different temperatures and adding structural stabilizers such as nanoclays (Laponite) and surfactants (Tegostab E-8158, E-8939). Taking advantage of the important plasticization relative to water, these rigid NIPU foams can be classified as SMMs triggered by humidity at room temperature. The hydrophilic hydroxyl groups in the NIPU network promote water uptake, which induces plasticization of the network, enhancing the flexibility of the polymer chains and allowing them to recover their original shape.

Overall, this work highlights the versatility and feasibility of using scCO_2 as a blowing agent for the fabrication of thermoset NIPU foams, offering a potential solution to valorize CO_2 not only for the synthesis of the precursors (cyclic carbonates) but also as a PBA during the foaming step. This process represents an innovative and efficient strategy to produce tailored NIPU foams with different morphological and mechanical properties for appealing applications. As a future perspective, the influence of scCO_2 conditions (P and T) during the impregnation step should be further investigated. Higher CO_2 uptake may reduce resin viscosity due to

plasticization, affecting the resin viscosity, foam expansion, and stability.

ASSOCIATED CONTENT

Supporting Information

The Supporting Information is available free of charge at <https://pubs.acs.org/doi/10.1021/acsapm.5c00494>.

Additional experimental details, ^1H NMR and FTIR spectra, gelation curves, additional images, DSC and TGA thermograms, and compressive stress–strain curves (PDF)

AUTHOR INFORMATION

Corresponding Authors

Sylvain Caillol – ICGM, ENSCM, CNRS, University of Montpellier, 34293 Montpellier, France; orcid.org/0000-0003-3106-5547; Email: sylvain.caillol@enscm.fr

Jean-Marie Raquez – Laboratory of Polymeric and Composite Materials (LPCM), University of Mons, 7000 Mons, Belgium; orcid.org/0000-0003-1940-7129; Email: jean-marie.raquez@umons.ac.be

Authors

Katherine Gouveia – Laboratory of Polymeric and Composite Materials (LPCM), University of Mons, 7000 Mons, Belgium; ICGM, ENSCM, CNRS, University of Montpellier, 34293 Montpellier, France; orcid.org/0009-0005-1651-6794

Joshua Vauloup – ICGM, ENSCM, CNRS, University of Montpellier, 34293 Montpellier, France

Maxime Colpaert – ICGM, ENSCM, CNRS, University of Montpellier, 34293 Montpellier, France

Connie Ocando – Laboratory of Polymeric and Composite Materials (LPCM), University of Mons, 7000 Mons, Belgium; orcid.org/0000-0003-4123-1879

Patrick Lacroix-Desmazes – ICGM, ENSCM, CNRS, University of Montpellier, 34293 Montpellier, France; orcid.org/0000-0002-0197-7062

Vincent Ladmiral – ICGM, ENSCM, CNRS, University of Montpellier, 34293 Montpellier, France; orcid.org/0000-0002-7590-4800

Complete contact information is available at: <https://pubs.acs.org/doi/10.1021/acsapm.5c00494>

Author Contributions

The manuscript was written through contributions of all authors. All authors have given approval to the final version of the manuscript.

Notes

The authors declare no competing financial interest.

ACKNOWLEDGMENTS

The authors would like to thank the financial support provided by the NIPU-EJD project. This project has received funding from the research and innovation program in the frame of European Union's Horizon 2022 under the Marie Skłodowska-Curie grant agreement No. 955700 (NIPU-EJD project). J.-M.R. is an FRS-FNRS Research Director and a WET-T investigator under the FRS-FNRS auspices.

REFERENCES

- (1) Engels, H. W.; et al. Polyurethanes: Versatile materials and sustainable problem solvers for today's challenges. *Angew. Chemie - Int. Ed.* **2013**, *52*, 9422–9441.
- (2) Szycher, M. *Szycher's handbook of polyurethanes*; CRC press, 1999.
- (3) Fraleoni-Morgera, A.; Afshani, M.; Montelpare, S.; Lops, C. Sustainable Micro- and Nanocomposites for Thermal Insulation in Buildings. *Adv. Eng. Mater.* **2023**, *26*, No. 2301064.
- (4) Gama, N. V.; Ferreira, A.; Barros-Timmons, A. Polyurethane foams: Past, present, and future. *Materials (Basel)* **2018**, *11*, 1841.
- (5) Peyrton, J.; Avérous, L. Structure-properties relationships of cellular materials from biobased polyurethane foams. *Mater. Sci. Eng. R Rep.* **2021**, *145*, No. 100608.
- (6) Singh, S. N. *Blowing agents for polyurethanes*; Rapra Technology, 2002.
- (7) Niaounakis, M. Chapter 9 - Foaming and Foamed Products. in *Biopolymers: Processing and Products*. ed., Niaounakis, M.; William Andrew Publishing, 2015, 327–359.
- (8) Polyurethane Foam Market, 2023. https://www.marketsandmarkets.com/Market-Reports/polyurethane-foams-market-1251.html?gad_source=1&gclid=CjwKCAiArfaUBhApEiwAeoB7qAVV3v7lev938U0f4O270DuoBWWc1ykHi87-95O-29QhQhYBLZ544BoCEbAQAvD_BwE.
- (9) *Climate change: what the EU is doing*, 2024. <https://www.consilium.europa.eu/en/policies/climate-change/>.
- (10) Cornille, A.; Auvergne, R.; Figovsky, O.; Boutevin, B.; Caillol, S. A perspective approach to sustainable routes for non-isocyanate polyurethanes. *Eur. Polym. J.* **2017**, *87*, 535–552.
- (11) Cornille, A.; Dworakowska, S.; Bogdal, D.; Boutevin, B.; Caillol, S. A new way of creating cellular polyurethane materials: NIPU foams. *Eur. Polym. J.* **2015**, *66*, 129–138.
- (12) Cornille, A.; et al. Room temperature flexible isocyanate-free polyurethane foams. *Eur. Polym. J.* **2016**, *84*, 873–888.
- (13) Coste, G.; Berne, D.; Ladmiraal, V.; Negrell, C.; Caillol, S. Non-isocyanate polyurethane foams based on six-membered cyclic carbonates ☆. *Eur. Polym. J.* **2022**, *176*, No. 111392.
- (14) Monie, F.; et al. Chemo- and Regioselective Additions of Nucleophiles to Cyclic Carbonates for the Preparation of Self-Blowing Non-Isocyanate Polyurethane Foams. *Angew. Chem.* **2020**, *132*, 17181–17189.
- (15) Bourguignon, M.; Grignard, B.; Detrembleur, C. Water-Induced Self-Blown Non-Isocyanate Polyurethane Foams. *Angew. Chem., -Int. Ed.* **2022**, *61*, No. e202213422.
- (16) Gunasekaran, H. B.; et al. Rapid Carbon Dioxide Foaming of 3D Printed Thermoplastic Polyurethane Elastomers. *ACS Appl. Polym. Mater.* **2022**, *4*, 1497–1511.
- (17) Belmonte, P.; et al. Transformation of TPU elastomers into TPU foams using supercritical CO₂. A new reprocessing approach. *J. Supercrit. Fluids* **2023**, *192*, No. 105806.
- (18) Wang, G.; et al. Structure-tunable thermoplastic polyurethane foams fabricated by supercritical carbon dioxide foaming and their compressive mechanical properties. *J. Supercrit. Fluids* **2019**, *149*, 127–137.
- (19) Villamil Jiménez, J. A.; et al. Foaming of PLA composites by supercritical fluid-assisted processes: A review. *Molecules* **2020**, *25*, 3408.
- (20) Nalawade, S. P.; Picchioni, F.; Janssen, L. P. B. M. Supercritical carbon dioxide as a green solvent for processing polymer melts: Processing aspects and applications. *Prog. Polym. Sci.* **2006**, *31*, 19–43.
- (21) Tomasko, D. L.; et al. A Review of CO₂ Applications in the Processing of Polymers. *Ind. Eng. Chem. Res.* **2003**, *42*, 6431–6456.
- (22) Grignard, B.; et al. CO₂-blown microcellular non-isocyanate polyurethane (NIPU) foams: From bio- and CO₂-sourced monomers to potentially thermal insulating materials. *Green Chem.* **2016**, *18*, 2206–2215.
- (23) Lemmon, E. W.; Bell, I. H.; Huber, M. L.; McLinden, M. O. Thermophysical Properties of Fluid Systems. in *NIST Chemistry WebBook*. eds., Linstrom, P. J.; Mallard, W. G.; National Institute of Standards and Technology (NIST)).
- (24) Coste, G.; Negrell, C.; Caillol, S. Cascade (Dithio)carbonate Ring Opening Reactions for Self-Blowing Polyhydroxythiourethane Foams. *Macromol. Rapid Commun.* **2022**.
- (25) Choong, P. S.; Hui, Y. L. E.; Lim, C. C. CO₂-Blown Nonisocyanate Polyurethane Foams. *ACS Macro Lett.* **2023**, *12*, 1094–1099.
- (26) Bacsik, Z.; et al. Mechanisms and kinetics for sorption of CO₂ on bicontinuous mesoporous silica modified with n-propylamine. *Langmuir* **2011**, *27*, 11118–11128.
- (27) Didas, S. A.; Sakwa-Novak, M. A.; Foo, G. S.; Sievers, C.; Jones, C. W. Effect of amine surface coverage on the Co-adsorption of CO₂ and water: Spectral deconvolution of adsorbed species. *J. Phys. Chem. Lett.* **2014**, *5*, 4194–4200.
- (28) Bose, M.; Nam, P. Role of additives in fabrication of soy-based rigid polyurethane foam for structural and thermal insulation applications. *J. Appl. Polym. Sci.* **2021**, *138*, No. 51325.
- (29) Monie, F.; Grignard, B.; Detrembleur, C. Divergent Aminolysis Approach for Constructing Recyclable Self-Blown Nonisocyanate Polyurethane Foams. *ACS Macro Lett.* **2022**, *11*, 236–242.
- (30) Pronoit, C.; Hakkarainen, M.; Odelius, K. Structurally Diverse and Recyclable Isocyanate-Free Polyurethane Networks from CO₂-Derived Cyclic Carbonates. *ACS Sustainable Chem. Eng.* **2022**, *10*, 2522–2531.
- (31) Blattmann, H.; Lauth, M.; Mülhaupt, R. Flexible and Bio-Based Nonisocyanate Polyurethane (NIPU) Foams. *Macromol. Mater. Eng.* **2016**, *301*, 944–952.
- (32) Leng, J.; Lu, H.; Liu, Y.; Huang, W. M.; Du, S. Shape-memory polymers - A class of novel smart materials. *MRS Bull.* **2009**, *34*, 848–855.
- (33) Huang, W. M.; et al. Shape memory materials. *Mater. Today* **2010**, *13*, 54–61.
- (34) Sessini, V.; Arrieta, M. P.; Fernández-torres, A.; Peponi, L. Humidity-activated shape memory effect on plasticized starch-based biomaterials. *Carbohydr. Polym.* **2018**, *179*, 93–99.
- (35) Sessini, V.; et al. Humidity-Activated Shape Memory Effects on Thermoplastic Starch/EVA Blends and Their Compatibilized Nanocomposites. *Macromol. Chem. Phys.* **2017**, *218*, No. 1700388.